Anisotropic electronic structure in quasi-one-dimensional $K_{0.3}MoO_3$: An angle-dependent x-ray absorption study

H. M. Tsai, K. Asokan,[a] C. W. Pao, J. W. Chiou, C. H. Du, and W. F. Pong[b]
Department of Physics, Tamkang University, Tamsui 251 Taiwan

M.-H. Tsai
Department of Physics, National Sun Yat-Sen University, Kaohsiung 804, Taiwan

L. Y. Jang
National Synchrotron Radiation Research Center, Hsinchu 300, Taiwan

(Received 18 January 2007; accepted 18 June 2007; published online 11 July 2007)

The electronic structure of quasi-one-dimensional (quasi-1D) blue bronze, $K_{0.3}MoO_3$, was investigated by angle-dependent x-ray absorption near-edge structure (XANES) spectroscopy at O and K *K* and Mo L_3 edges along the quasi-1D MoO_6 octahedron-chain direction, i.e., the ***b*** axis, and the octahedron-in-plane direction, i.e., the ***d*** axis, well below its Peierls phase transition temperature (180 K). The O *K*-edge XANES spectra indicate that the angle dependence of O $2p$–Mo $4d$ hybridization, especially those with the π^* character, is more significant along the ***b*** axis than along the ***d*** axis. Similar trend is also observed in the Mo L_3-edge XANES spectra. The K *K*-edge XANES spectra reveal anisotropic effect of hybridization of K $4p$ states with O $2p$ states on the MoO_6 octahedron. © *2007 American Institute of Physics*. [DOI: 10.1063/1.2756358]

Molybdenum bronzes belong to a class of solid oxides with intense color and metallic luster.[1] Of these, $K_{0.3}MoO_3$ (KMO) is a prototype blue bronze that exhibits quasi-one-dimensional (quasi-1D) electron transport property and a metal-semiconductor transition to a charge-density-wave (CDW) phase at 180 K.[1–4] Electrical, magnetic, and optical properties are strongly anisotropic with quasi-1D behavior. Hence, this material has been investigated using various experimental approaches to understand the origin of these properties. Its electrical conductivity is an order of magnitude larger along the chain (***b*** axis) than along the octahedron-in-plane (***d*** axis) direction and it is very sensitive to the thermodynamical parameters.[1–4] A detailed understanding of the direction-dependent electronic structure is critical to elucidate the anisotropic behavior of KMO. Such a study will also provide information on the electronic states of O and Mo atoms and the role played by K atoms in its anisotropic electronic properties, which has not been revealed in previous experimental and theoretical investigations.[1–6]

KMO has a centered monoclinic structure and contains MoO_6 chains with K atoms residing between adjacent chains. KMO has 20 f.u. in a unit cell, which has ten distorted MoO_6 octahedra that share edges or corners in a cluster (see Fig. 1)[1,3,7,8] These clusters are connected through three nonequivalent Mo sites in the KMO structure. The Mo(1) octahedron shares its edges and corners with only the Mo(2) and Mo(3) octahedra of the same unit cell. These clusters are linked together by sharing corners along and perpendicular to the ***b*** axis and form into chains. There are two nonequivalent K sites. The vector $\boldsymbol{d}=2\boldsymbol{c}+\boldsymbol{a}$, where ***c*** and ***a*** are the lattice parameters, is perpendicular to the ***b*** axis. The unit cell in blue bronze is spanned by vectors ***b*** and ***d***.[7,8]

When spectroscopic measurements are made along these two axes, the anisotropy can be identified. X-ray absorption near-edge structure (XANES) is an element specific probe that is sensitive to local structure around the absorbing atom and to the coordination geometry of its near neighbors. Linear polarization-dependent XANES can be employed to probe selectively the symmetry of the final states relative to the various crystallographic directions. Duda *et al.*[7] and Sing *et al.*[8] adopted this approach to understand the electronic structure of KMO. Huang *et al.* investigated this compound using the same technique, by varying the temperature and the applied voltage, to elucidate O $2p$–Mo $4d$ hybridized states and the effect of the local atomic structure associated with the dynamic CDW of KMO.[9] This work uses angle-dependent XANES spectroscopy to probe the electronic structures at O, Mo, and K sites, along the ***b*** and ***d*** axes, respectively, by the photoexcitation of electrons from discrete core levels to states above the Fermi level. These mea-

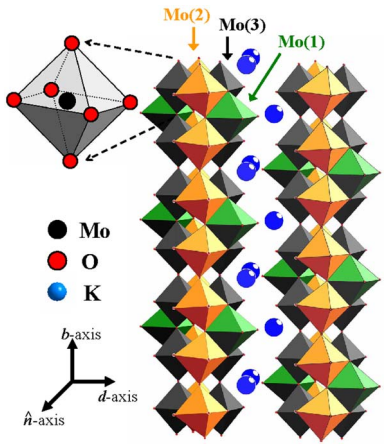

FIG. 1. (Color online) Crystal structure of the prototype blue bronze, $K_{0.3}MoO_3$; nonequivalent Mo sites are denoted by Mo(1), Mo(2), and Mo(3). The zigzag chain structure of K ions is also evident.

[a]Permanent address: Inter University Accelerator Center, Aruna Asaf Ali Marg, New Delhi 110 067, India.
[b]Author to whom correspondence should be addressed; electronic mail: wfpong@mail.tku.edu.tw

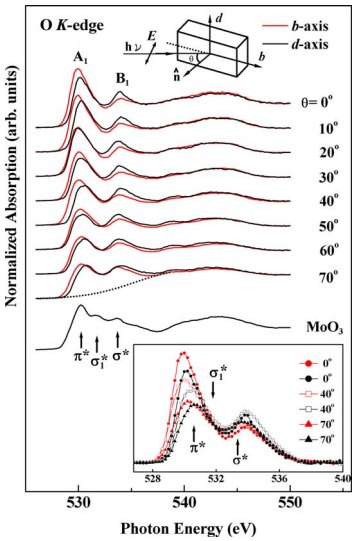

FIG. 2. (Color online) Normalized XANES spectra at the O *K* edge measured at various angles and along the ***b*** and ***d*** axes obtained at 140 K. The top inset presents the geometry of measurement and the bottom inset magnifies the variation in spectral features at various angles, θ=0°, 40°, and 70°, and along the ***b*** and ***d*** axes.

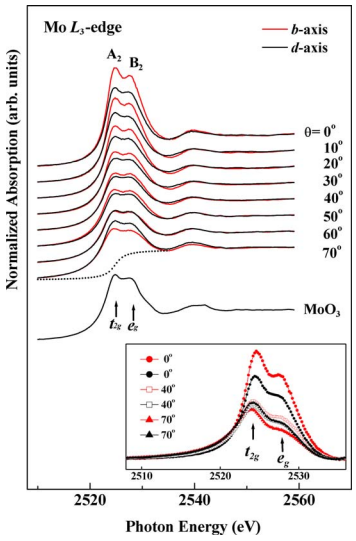

FIG. 3. (Color online) Normalized XANES spectra at the Mo L_3 edge measured at various angles and along the ***b*** and ***d*** axes obtained at 140 K. The inset magnifies the variation in the $4d$ t_{2g} and e_g bands at various angles, θ=0°, 40°, and 70°, and along the ***b*** and ***d*** axes.

surements provide a site-specific probe of the symmetry of unoccupied states and yield information on the local environments at O, Mo, and K sites in the CDW phase of the KMO.

The angle-dependent XANES spectra were obtained at the National Synchrotron Radiation Research Center, Hsinchu, Taiwan. The KMO single crystal was grown using a temperature gradient flux technique and its orientation was determined by x-ray diffraction.[10] A rectangular piece of crystal with an area of $\sim 2\times 3$ mm^2 was prepared and the longer side of the rectangle was aligned with the ***b*** axis of the crystal. All these measurements were carried out at 140 K with a temperature stability of ±1 K using a continuous flow-type helium cryostat; this temperature was well below the Peierls phase transition temperature of 180 K of KMO.

Figure 2 displays the normalized O *K*-edge XANES spectra of KMO and reference MoO_3 along both the ***b*** and ***d*** axes at angles of 0°–70°. The upper part of the inset in Fig. 2 presents the experimental geometry used in this work, in which ***E*** is the polarization of the incoming photons and θ is the incidence angle. These spectral features are consistent with the reports available in the literature.[7–9] The O *K*-edge XANES spectra reflect transitions from the O $1s$ core state to the unoccupied O $2p$ derived states and the states of neighboring atoms, which have p-symmetry components projected onto the O sites. The positions of the spectral features agree with those of the calculated partial densities of states of KMO using the first-principles method.[6] The two prominent features (A_1 and B_1) near 530 and 534 eV are known to correspond to the unoccupied π^* and σ^* bands formed by hybridization between O $2p_\pi$ and Mo $4dt_{2g}$ states and between O $2p_\sigma$ and Mo $4de_g$ states,[7–9] respectively. The shoulder (σ_1^*) at ~532 eV from the reference compound, MoO_3, is associated with the anisotropy of the Mo $4dt_{2g}$ band due to the presence of nonequivalent oxygen atoms in the first coordination shell,[11,12] which is not clearly observed in the spectra of KMO. This result reveals that the environments of O ions differ from those in MoO_3. The hybridization of the K $4sp$–O $2p$ states reduces the number of unoccupied states of anisotropic O $2p$-$4dt_{2g}$ bands centered at ~532 eV in the KMO spectra and broadens feature B_1. The broad humplike feature from ~537 to 546 eV was attributed to Mo $5sp$–O $2p$ hybridized states.[7,8,11] The lower inset in Fig. 2 presents magnified near-edge features in the θ=0°, 40°, and 70^0 spectra along the ***b*** and ***d*** axes after subtraction of the Gaussian background indicated by the dashed line in Fig. 2. As revealed in the inset, the intensity of the π^* feature is highest at θ=0° and decreases to a minimum at θ=70° as the angle increases; the intensity of the σ^* feature varies oppositely. In ***d***-axis spectra, π^* features slightly shift to higher energies and have a similar trend as those in the ***b*** axis spectra. However, the intensity of the σ^* feature does not show a clear trend. The difference intensities between ***b***- and ***d***-axis spectra are substantially larger for smaller angles than those for larger angles, because at small angles the ***E*** field of photons are predominantly parallel with the ***b*** axis and along the ***b*** axis O *K*-edge measurement probes a larger number of Mo–O hybridized states due to a larger number of Mo–O bonds along the chain, while along the ***d*** axis the MoO_6 clusters are separated by K ions and consequently O *K*-edge measurement probes a smaller number of Mo–O bonds and Mo–O hybridized states.

Figure 3 displays normalized Mo L_3-edge XANES spectra of KMO and reference MoO_3 at various angles along the ***b*** and ***d*** axes. Spectral features A_2 and B_2 reflect transitions from Mo $2p_{3/2}$ to $4d$ orbitals and provide information about unoccupied Mo $4d$-derived states.[13] As shown in the figure, the white lines clearly split into $4dt_{2g}$ and $4de_g$ bands. The difference between the spectral features of KMO and MoO_3 indicates that MoO_6 octahedra are distorted by the insertion of K atoms between MoO_6 chains, which broadens both t_{2g} and e_g bands. The lower inset in Fig. 3 presents magnified near-edge features in the spectra of θ=0°, 40°, and 70° along the ***b*** and ***d*** axes, in which the intensities of the white line feature were subtracted with a fitted arctangent function of the continuum step centered at the position of the maximum height, as indicated by the dashed line in Fig. 3. The intensities of the features for the ***b***- and ***d***-axis cases decrease with the increase of θ. The rate of change of the intensity with respect to θ is much larger for the ***b*** axis case than for the

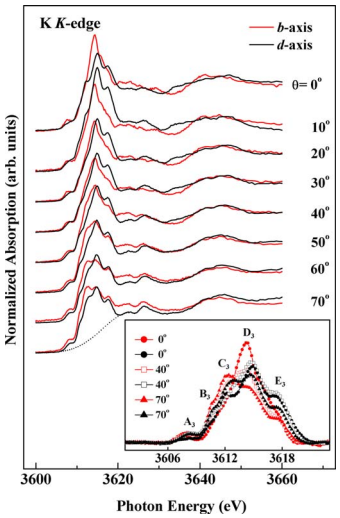

FIG. 4. (Color online) Normalized XANES spectra at the K *K* edge measured at various angles and along the ***b*** and ***d*** axes obtained at 140 K. The inset magnifies the variation in spectral features at various angles, $\theta=0°$, 40°, and 70°, and along the ***b*** and ***d*** axes.

d-axis case such that at $\theta=0°$ the intensity for the ***b***-axis case is the largest, while at $\theta=70°$ it is the smallest. This trend is consistent with that of the near-edge features at the O *K* edge and is originated from the same anisotropic structural property.

The MoO_6 octahedra and the double ReO_3-type chains are common to MoO_3 and KMO,[8] implying that the quasi-1D electronic property of KMO may originate from the quasi-1D zigzag chain of K atoms inserted between MoO_6 chains. Therefore, XANES at the K *K* edge is important to understand the nature of the quasi-1D electronic property. Figure 4 displays the normalized XANES spectra at the K *K* edge of KMO measured at various angles for the ***b***- and ***d***-axis cases. These spectral features are very similar to those observed in other alkali metals and potassium-based compounds.[14,15] Since the electronic state transitions originate from the K 1*s* core level, only the states with p_{xy} (σ^* band) and p_z (π^* band) symmetries centered at the K site are relevant. The inset in Fig. 4 presents magnified near-edge features of $\theta=0°$, 40°, and 70° for both the ***b***- and ***d***-axis cases following subtraction of the Gaussian background indicated by the dashed line shown in Fig. 4. A weak preedge feature A_3 (at ~3608 eV) was attributed to a *dipole forbidden* K 1*s* transition to 4*s* that hybridizes with O 2*p* states and the sharp spectral features B_3 (at ~3610 eV), C_3 (at ~3612 eV), D_3 (at ~3615 eV), and E_3 (~3618 eV) in the spectra were attributed to transitions from the 1*s* to the 4*p* states of K by Teodorescu *et al.*[14] and Marcelli *et al.*[15] The inset in the figure presents the variation of the intensities of these spectral features at various angles for the ***b***- and ***d***-axis cases. The changes in the spectral features can be understood by considering that K $4p_{xy}$ (B_3 and C_3) and K $4p_z$ (D_3 and E_3) bands are preferentially probed at large and small incidence angles, respectively, so that along the ***b*** axis, features D_3 and E_3 have maximum intensity at $\theta=0°$ and B_3 and C_3 have maximum intensity at $\theta=70°$. Along the ***d*** axis, the features B_3 and C_3 have similar angle dependence as in the ***b*** axis. However, features D_3 and E_3 do not show a clear trend because their intensities are largest at $\theta=40°$, which may be due to the two nonequivalent K sites in the zigzag chain, as shown in Fig. 1. We have also compared the spectral features with those measured at room temperature above the Peierls transition temperature (not shown here), which shows that peak A_3 does not have significant variation with temperature in both axes, indicating that the dipole-forbidden transition is allowed because of hybridization, not phonon coupling.

The above angle-dependent XANES spectra at the K *K* edge of KMO show more significant variations in the intensity, general line shape and energy position than those at the O *K* and Mo L_3 edge, which suggests that the anisotropy of this compound is strongly related to inserted K atoms. The B_3 and C_3 features associated with K $4p_{xy}$ orbitals in the K *K*-edge XANES spectra have similar angle dependence as those of the O *K*-edge XANES spectra, which suggests hybridization between K 4*p* and O 2*p* orbitals. Since cation K has a much smaller electronegativity than cation Mo, K atoms are expected to donate electrons and significantly modify charge transfer in the MoO_3 host system and this effect is anisotropic due to the zigzag chain structure of K ions. The inserted K atoms also give rise to an altered ligand field, which splits K 4*p* states into two components, σ^* and π^*, and thus alters Mo $4d-O\ 2p$ hybridized bands.

In summary, this work employed angle-dependent XANES, which is extremely sensitive to both the geometry and the chemical interlayer of the ionic environment, to demonstrate that significant anisotropy in the electronic properties of KMO by comparing the spectral details of the K *K* edge with those of the O *K* and Mo L_3 edges. The alkali ions K are found to cause asymmetry in the crystal field of Mo through anisotropic hybridization with O ions in the octahedron due to the quasi-1D zigzag chain structure of K ions inserted between host MoO_3 chains.

This work was supported by the National Science Council of Taiwan under Contract No. NSC 95-2112-M-032-014.

[1] *Low Dimensional Electronic Properties of Molybdenum Bronzes and Oxides*, edited by C. Schlender (Kluwer, Dordrecht, 1989).
[2] G. Gruner, Rev. Mod. Phys. **60**, 1129 (1988); G. Gruner, *Density Waves in Solids* (Addison-Wesley, Longmans, MA, 1994).
[3] R. E. Thorne, Phys. Today **49**, 42 (1996).
[4] M. Greenblatt, Chem. Rev. (Washington, D.C.) **88**, 31 (1988).
[5] G. K. Wertheim, L. F. Schneemeyer, and D. N. E. Buchanan, Phys. Rev. B **32**, 3568 (1985).
[6] J. L. Mozos, P. Ordejón, and E. Canadell, Phys. Rev. B **65**, 233105 (2002).
[7] L. C. Duda, J. H. Guo, J. Nordgren, C. B. Stagarescu, K. E. Smith, W. McCarroll, K. Ramanujachary, and M. Greenblatt, Phys. Rev. B **56**, 1284 (1997).
[8] M. Sing, R. Neudert, H. von Lips, M. S. Golden, M. Knupfer, J. Fink, R. Claessen, J. Mücke, H. Schmitt, S. Hüfner, B. Lommel, W. Aβmus, Ch. Jung, and C. Hellwig, Phys. Rev. B **60**, 8559 (1999).
[9] C. H. Huang, J. C. Jan, J. W. Chiou, H. M. Tsai, C. W. Pao, C. H. Du, W. F. Pong, M.-H. Tsai, M. T. Tang, J. J. Lee, and J. F. Lee, Appl. Phys. Lett. **86**, 141905 (2005).
[10] C. H. Du, Y. R. Lee, C. Y. Lo, H. H. Lin, S. L. Chang, M. T. Tang, Y. P. Stetsko, and J. J. Lee, Appl. Phys. Lett. **88**, 241916 (2006).
[11] J. Purans, A. Kuzmin, Ph. Parent, and C. Laffon, Electrochim. Acta **46**, 1973 (2001).
[12] C. A. Rozzi, F. Manghi, and F. Parmigiani, Phys. Rev. B **68**, 075106 (2003).
[13] E. J. Lede, F. G. Requejo, B. Pawelec, and J. L. G. Fierro, J. Phys. Chem. B **106**, 7824 (2002).
[14] C. M. Teodorescu, A. El Afif, J. M. Esteva, and R. C. Karnatak, Phys. Rev. B **63**, 233106 (2001).
[15] A. Marcelli, G. Cibin, G. Cinque, A. Mottana, and M. F. Brigatti, Radiat. Phys. Chem. **75**, 1596 (2006).